



ELSEVIER

Available online at www.sciencedirect.com

SCIENCE @ DIRECT®

Nuclear Instruments and Methods in Physics Research A 525 (2004) 126–131

**NUCLEAR
INSTRUMENTS
& METHODS
IN PHYSICS
RESEARCH**
Section A

www.elsevier.com/locate/nima

In-beam tests of the AMS RICH prototype with 20 A GeV/ c secondary ions

B. Baret^{a,*}, P. Aguayo^b, M. Aguilar Benitez^b, L. Arruda^c, F. Barao^c, A. Barrau^a,
E. Belmont^d, J. Berdugo^b, G. Boudoul^a, J. Borges^c, M. Buénerd^a, D. Casadei^e,
J. Casaus^b, C. Delgado^b, C. Diaz^b, L. Derome^a, L. Eraud^a, L. Gallin-Martel^a,
F. Giovacchini^e, P. Goncalves^c, E. Lanciotti^b, G. Laurenti^e, A. Malinine^f,
C. Mana^b, J. Marin^b, G. Martinez^b, A. Menchaca-Rocha^d, C. Palomares^b,
M. Pimenta^c, K. Protasov^a, E. Sanchez^b, E-S. Seo^a, I. Sevilla^b,
A. Torrento^b, M. Vargas-Trevino^a

^aLPSC, Avenue des Martyrs 53, F-38026 Grenoble-cedex, France

^bCIEMAT, Avenida Complutense 22, E-28040 Madrid, Spain

^cLIP, Avenida Elias Garcia 14-1, P-100 Lisboa, Portugal

^dInstituto de Física, UNAM, AP 20-364, Mexico DF, Mexico

^eUniversity of Bologna and INFN, Via Irnerio 46, I-40126 Bologna, Italy

^fUniversity of Maryland, College Park, MD 20742, USA

Abstract

A prototype of the AMS Cherenkov imager (RICH) has been tested by means of a low intensity 20 GeV/ c per nucleon ion beam coming from the fragmentation of a primary beam of Pb ions. Data have been collected for charges $1 < Z < \sim 45$ in various beam conditions and using different radiators. The charge Z and velocity β resolution have been of the prototype investigated.

© 2004 Elsevier B.V. All rights reserved.

PACS: 29.40. Ka

Keywords: AMS experiment; RICH; In-beam tests; Fragmentation beam

1. Introduction

The AMS spectrometer will be installed on the International Space Station in the year 2006, for a several years campaign of measurements during

which a research program of fundamental interest will be covered: Search for antimatter of primordial origin, for dark matter, study of the Cosmic Ray flux (CR) and gamma-ray astronomy. The Cherenkov imager of the experiment should make possible a thorough study of the nuclear Cosmic Ray flux by performing: (a) isotope identification (ID) for the light elements over a range of mass (A) and momentum (P) of about

*Corresponding author.

E-mail address: baret@lpsc.in2p3.fr (B. Baret).

¹On behalf of the AMS-RICH collaboration.

($A < \sim 15-20$, $1 \text{ GeV}/c < P/A < \sim 12 \text{ GeV}/c$), and (b) charge measurements of the particles with charge resolution of the order of one unit up to Fe ($Z < \sim 26$), the momentum range extending up to the upper limit of the spectrometer capability, in the TeV/c per nucleon range, $P/A < \sim 1 \text{ TeV}/c$.

The technical requirements constraining the imager design (dimensions, weight, power consumption, long-term reliability of photodetectors) have lead to the choice of a proximity focusing type of imager, equipped with multianode photomultipliers for photon detection. The radiators were chosen in accordance with the physics requirements and ID capabilities of the counter: Sodium fluoride (NaF) and silica aerogel, to cover the low ($1 \text{ GeV}/c < P/A < \sim 5 \text{ GeV}/c$) and high ($4 \text{ GeV}/c < P/A < \sim 12 \text{ GeV}/c$) parts of the momentum range, respectively.

2. RICH architecture

The mechanical structure of the imager is shown in Fig. 1. It consists of a radiator plane at the top, separated from the photodetector plane by a 45 cm drift space. The empty area in the detector plane corresponds to the location of the electro-

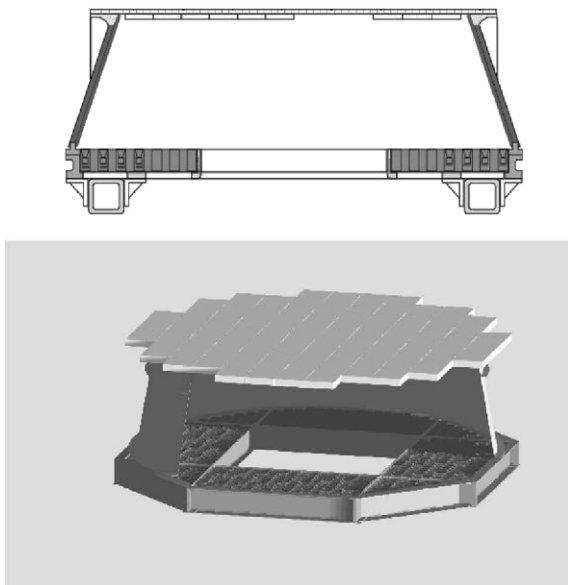


Fig. 1. Structure of the final imager.

magnetic calorimeter. A conical mirror encloses the drift volume to increase the acceptance. The detector plane includes 680 PMTs, corresponding to 10880 read-out channels. The Cherenkov radiator plane will be equipped with NaF ($n = 1.33$) in the central region ($\sim 35 \times 35 \times 0.5 \text{ cm}^3$) and silica aerogel ($n = 1.03-1.05$, 3 cm thick) in the rest of the area.

3. Prototype and setup

The prototype (Fig. 2) consists of a fraction of the detector in a version close to the flight model design. This comprises 96 cells of photodetectors. Each cell includes, mounted altogether and enclosed in a plastic shell (Fig. 3): a 16-anode Hamamatsu R7900_M16 PMT, a 16-element light guide matrix, a HV divider, the analogic frontend electronics and analogic to digital converter. The ASIC has been especially developed and designed for the detector [1]. Each element is inserted in a

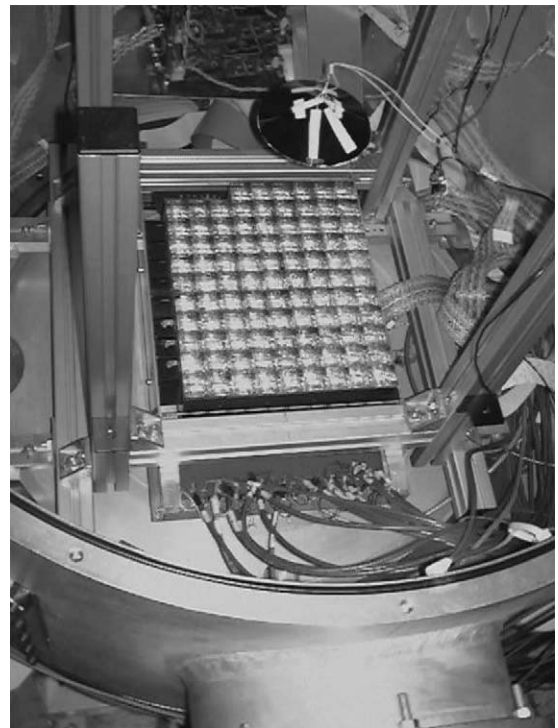


Fig. 2. Prototype matrix in its light tight box.

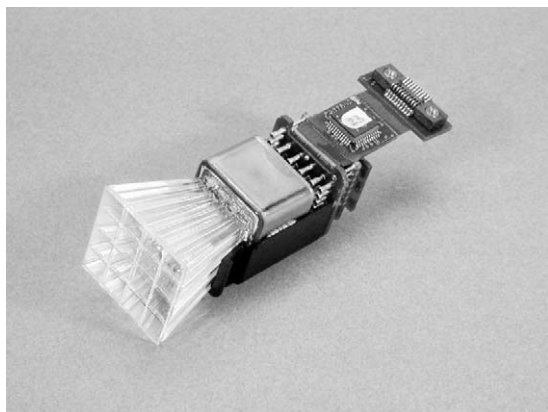


Fig. 3. One PMT module with light guide, electronics and half plastic shell.

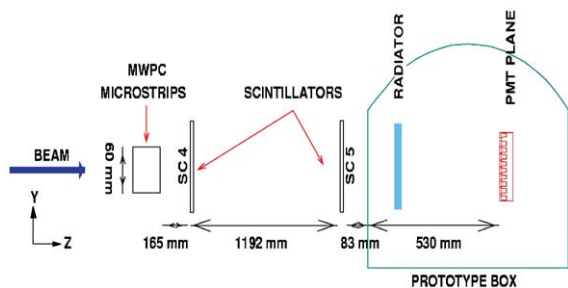


Fig. 4. Experimental setup on the beam line.

magnetic shielding grid. The DAQ systems reads out 1536 channels in total. The whole thing was put in a light tight box. The detection setup was completed with a hybrid multiwire proportional chamber detector with delay line readout for beam localisation and two dE/dX plastic scintillators for independent charge measurement (Fig. 4). The prototype was tested with a set of different aerogel radiators with refractive index $1.03 < n < 1.05$ from two manufacturers, Matsushita Electric Co. (MEC) [2] and Catalysis Institute of Novosibirsk (CIN) [3].

4. The CERN SPS test beam

The beam was obtained from the CERN SPS by fragmentation of primary Pb ions on a production target (10 cm Be or 40 cm Pb) located at the

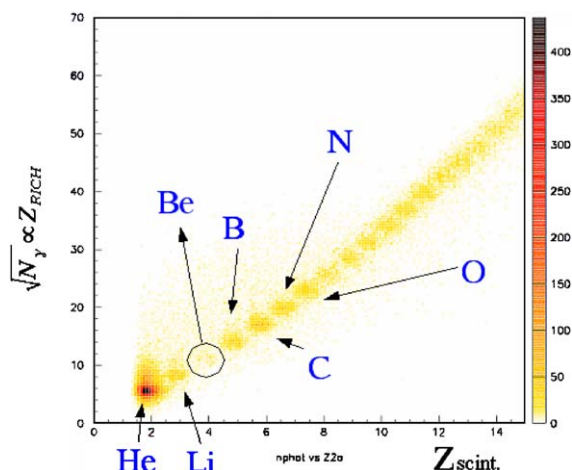


Fig. 5. Correlation between a dE/dX scintillator and the square root of the number of Cherenkov photons.

entrance of the beam line. The secondary beam intensity was set to about $1\text{--}3 \times 10^3$ particles per spill. The beam line was operated as a magnetic spectrometer and used to select samples of ions with a given rigidity. The fragmentation products fly to a good approximation at the beam velocity γ_b , and only particles entering the beam line with a ratio A/Z matching the rigidity settings for the beam line $B\rho = 3.1\gamma_b A/Z$, were transported to the detector. The most useful ratio $A/Z = 2$ provided a secondary beam including the whole range of nuclear masses: ${}^2\text{H}$, ${}^4\text{He}$, ${}^6\text{Li}$, ${}^{10}\text{B}$, ${}^{12}\text{C}$, ${}^{14}\text{N}$, ${}^{16}\text{O}$, ..., ${}^{28}\text{Si}$, ..., ${}^{40}\text{Ca}$, ..., ${}^{52}\text{Fe}$, ... etc., produced by projectile fragmentation. Other more selective field settings have been used to pick $A/Z \neq 2$ isotope ratios, like $\frac{3}{2}$ for ${}^3\text{He}$ and $\frac{7}{4}$ for ${}^7\text{Be}$. Fig. 5 shows the ions seen for the $A/Z = 2$ setting through the correlation between the charge measured by a scintillator and the square root of the number of Cherenkov photoelectrons (proportional to Z). Details on the beam design and performances are given in Ref. [4].

5. Results

Cherenkov rings associated to the beam ions over the covered range of charge have been observed, with the number of photons ranging

from 4–7 (mean value depending on the radiator sample) for $Z = 1$ elements, up to several thousands for high Z values. Fig. 6 shows a sample of rings for different charges obtained with the 1.03 MEC aerogel radiator. The central pattern is due to Cherenkov light created by the incident particle passing through the light guides. The charge and velocity resolutions are being evaluated from the analysis of the 5 million events recorded.

5.1. Velocity measurement

The velocity reconstruction was made using two types of algorithms. The first one uses the trace of the particle in the MWPC to calculate a Cher-

enkov angle for each hit on the matrix. This provides a cluster of similar angle values corresponding to the Cherenkov ring plus scattered background hits. This method is mostly used for protons which produce too few photons (typically around 6) to use the second algorithm. The latter is based on geometrical fitting of a ring pattern and is more efficient for large number of hits.

The velocity (β) resolution was found in agreement with former cosmic rays tests estimates (see Ref. [5]), i.e., around $\Delta\beta/\beta \sim 10^{-3}$ for $Z = 1$ particles. For larger Z values, the resolution first decreases (improves) as Z^{-1} for $Z < 7$ as observed previously [6], then starts decreasing progressively slower than Z^{-1} up to $Z \sim 25$,

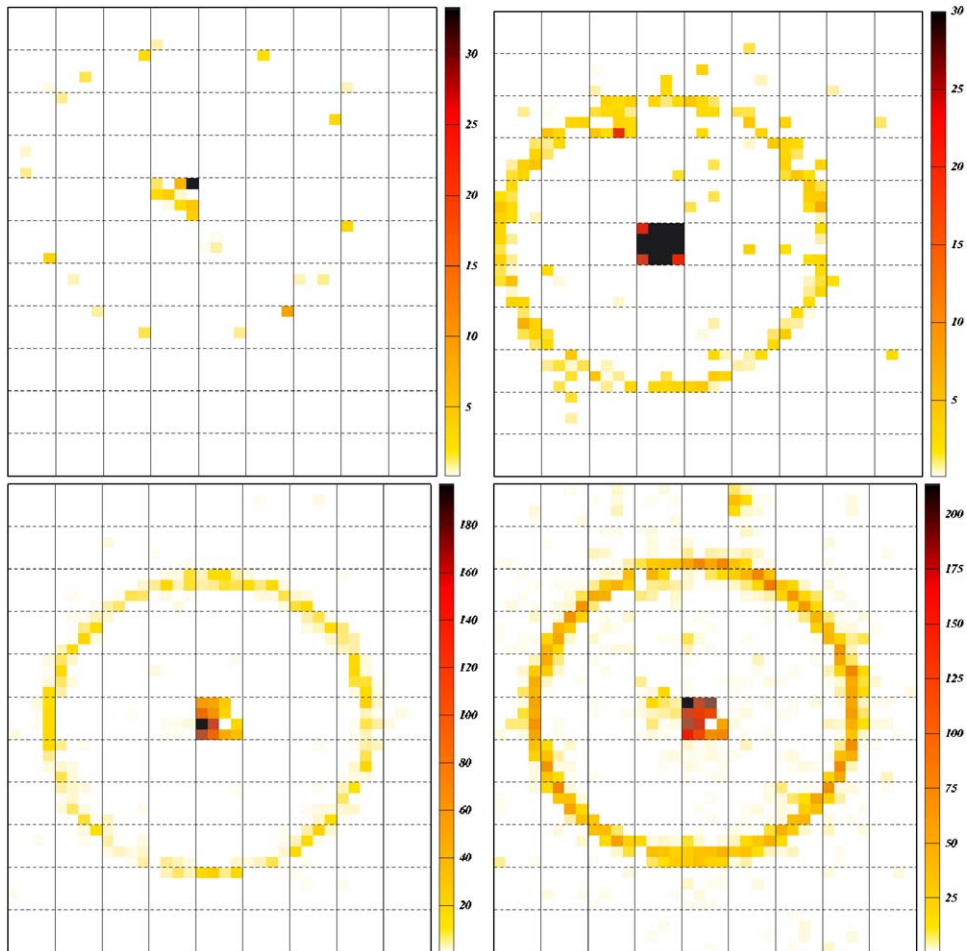


Fig. 6. Ring patterns for $Z = 2$ (top left), 6 (bottom left), 10 (top right) and around 26 (bottom right).

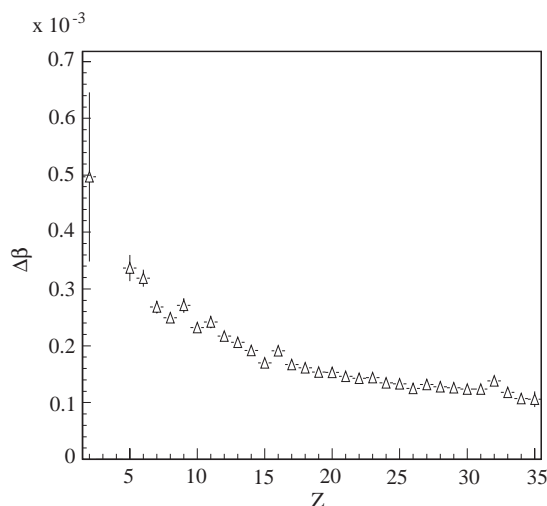


Fig. 7. Velocity resolution vs. charge.

flattening above this value to a Z independent, constant value, according to the relation $\sigma(\beta) = 10^{-4} \sqrt{(\sim 10/Z)^2 + (\sim 1)^2}$ (see Fig. 7 for MEC aerogel 1.03 data). The constant term limitation is set by the pixel size of the detector plane.

5.2. Charge measurement

A realistic evaluation of the isotope separation capability of the final counter will be produced from this analysis. Fig. 8 shows the preliminary analysis results of the prototype performance for Z measurement with 3.1 cm thick $n = 1.04$ CIN aerogel.

The charge reconstruction uses the estimator $Z_{\text{meas}} = \sqrt{N_{\text{ring}}/N_{\text{exp}}}$ where N_{ring} is the number of photoelectrons detected in the ring and N_{exp} is the expected number of photoelectrons for a $Z = 1$ particle calculated thanks to a Monte Carlo simulation. The measured resolution in Z is of the order of $\sigma(Z) = 0.3$ in the region of Fe ($Z = 26$), in fair agreement with the estimates. Although the dynamic range goes beyond, and although higher Z data have been recorded in the run, up to around $Z = 45$, the study of upper Z range suffers from the lack of good external Z measurements. The work is in progress.

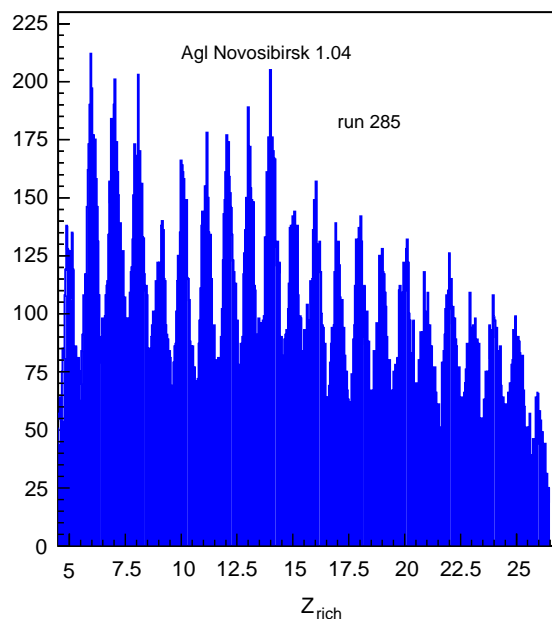
Fig. 8. Charge reconstruction for $n = 1.04$ CIN Aerogel.

Table 1
 β resolution and Clarity coefficient measured for the tested radiators

| Radiator | Index | Resolution ($\times 10^3$) | Clarity ($\text{m}^4 \text{cm}^{-1}$) |
|----------|-------|------------------------------|---|
| MEC | 1.03 | 0.71 ± 0.02 | 0.0079 ± 0.0001 |
| MEC | 1.05 | 0.98 ± 0.05 | 0.0095 ± 0.0002 |
| CIN | 1.04 | 0.94 ± 0.08 | 0.0120 ± 0.0002 |
| CIN | 1.03 | 0.67 ± 0.01 | 0.0059 ± 0.0001 |

5.3. Radiators selection

The different radiators have been evaluated on the two criteria of velocity and charge resolution. The material clarity is a key property for this selection. In addition, giving priority to the β or Z resolution and considering the reconstruction efficiency for $Z = 1$ particle may lead to the choice of a small (1.03) or large (1.05) refractive index value. The best radiator appears to be the $n = 1.03$ CIN (see Table 1). However, the hydrophilic properties of this material could make the integration of the final detector more complex. This issue is currently being investigated considering that the $n = 1.03$ MEC also shows good properties.

6. Conclusions and perspectives

These in-beam test of the RICH imager prototype of the AMS spectrometer have validated the instrumental and analysis solutions. The velocity and charge resolution of the instrument have been found to provide the expected performances. The properties of different radiators have been investigated in view of the final choice for the flight model of the imager.

References

- [1] L. Gallin-Martel, et al., Nucl. Instr. and Meth. A 504 (2003) 273.
- [2] Matsushita Electric Works, Ltd., 1048 Kadoma, Osaka 571-8686, Japan.
- [3] Borekov Institute of Catalysis, Pr.Akademika Lavrentieva, 5 Novosibirsk, Russia, 630090.
- [4] M. Buénerd, I. Efthymiopoulos. Report CERN-AB-2003.
- [5] T. Thuillier, et al., Nucl. Instr. and Meth. A 491 (2002) 83.
- [6] J. Casaus, et al., The AMS RICH collaboration, Nucl. Phys. B 113 (2002) 147;
M. Buénerd, et al., Nucl. Instr. and Meth. A 502 (2003) 158.